MOLECULAR AND CELLULAR BIOLOGY, Feb. 1999, p. 1450–1459 Vol. 19, No. 2
0270-7306/99/$04.00+0

Studies of Human MDR1-MDR2 Chimeras Demonstrate the Functional Exchangeability of a Major Transmembrane Segment of the Multidrug Transporter and Phosphatidylcholine Flippase

YI ZHOU,[1] MICHAEL M. GOTTESMAN,[2] AND IRA PASTAN[1]*

Laboratory of Molecular Biology[1] and Laboratory of Cell Biology,[2] National Cancer Institute, National Institutes of Health, Bethesda, Maryland 20892

Received 31 July 1998/Returned for modification 23 September 1998/Accepted 6 November 1998

P-glycoprotein (P-gp), encoded by the *MDR1* gene, is a plasma membrane transporter which effluxes a large number of structurally nonrelated hydrophobic compounds. The molecular basis of the broad substrate recognition of P-gp is not well understood. Despite the 78% amino acid sequence identity of the *MDR1* and *MDR2* transporter, MDR2, which has been identified as a phosphatidylcholine transporter, does not transport most MDR1 substrates. The structural and functional differences between MDR1 and MDR2 provide an opportunity to identify the residues essential for the broad substrate spectrum of MDR1. Using an approach involving exchanging homologous segments of MDR1 and MDR2 and site-directed mutagenesis, we have demonstrated that MDR1 residues Q330, V331, and L332 in transmembrane domain 6 are sufficient to allow an MDR2 backbone in the N-terminal half of P-gp to transport several MDR1 substrates, including bisantrene, colchicine, vinblastine, and rhodamine-123. These studies help define some residues important for multidrug transport and indicate the close functional relationship between the multidrug transporter (MDR1) and phosphatidylcholine flippase (MDR2).

Expression of the multidrug transporter P-glycoprotein (P-gp) is one of the major causes of multidrug resistance in cancer cells. P-gp is a 170-kDa membrane protein encoded by the MDR1 gene in humans. Based on its sequence and domain organization, P-gp is classified as a member of ATP binding cassette superfamily; it consists of two symmetrical halves, each half containing six transmembrane (TM) domains and a cytoplasmic nucleotide binding domain. Although most members of the ABC transporter family have stringent substrate specificities, P-gp recognizes many compounds, including anthracyclines (e.g., doxorubicin and daunomycin), vinca alkaloids (e.g., vincristine and vinblastine), antibiotics (e.g., actinomycin D), circular and toxic peptides (e.g., valinomycin and gramicidin), and relatively noncytotoxic agents such as verapamil, azidopine, quinidine, and cyclosporin A. These P-gp substrates have no common chemical structure. They are all low-molecular-weight nonanionic hydrophobic or amphipathic compounds (11).

Although a detailed understanding of the molecular basis of P-gp substrate specificity must await high-resolution three-dimensional protein structure analysis, much information can be obtained through mutational studies aimed at analyzing the regions of homology and nonhomology between MDR molecules from the different species. Two MDR homologs, MDR1 and MDR2, have been identified in humans. Despite MDR2 having a 78% overall amino acid sequence identity and a domain organization predicted to be the same as MDR1 (32), MDR2 protein is a phosphatidylcholine transporter which recognizes some other phospholipids (30, 31). However, the MDR2 transporter does not confer drug resistance in a broad spectrum. Photoaffinity labeling experiments have shown that the inability of the mouse mdr2 transporter to confer resistance to specific drugs is associated with reduced binding of these drugs to the mdr2 protein (4). Studies of MDR1-MDR2 chimeric proteins show that exchanging ATP binding domains between MDR1 and MDR2 results in few changes in the function of MDR1; however, exchanging the homologous segments containing a few TM regions abrogates the capacity of the MDR1 transporter to confer multidrug resistance (3, 7, 34). The loss of multidrug transporter function in the chimeric P-gp can be partially restored through selectively changing a few MDR2 residues back to MDR1 residues, indicating that not all of the nonidentical residues contribute equally to the differences in transport function between MDR1 and MDR2 (7). Since MDR1 and MDR2 proteins have a similar domain structure and they both transport hydrophobic and amphipathic substrates, their substrate preferences are most likely determined by some of the nonidentical residues within the MDR protein transmembrane domains. Identification of these residues will help reveal the molecular basis of the specific interaction between P-gp and its substrates.

In this work, we have focused on the residues around TM domain 6 (TM6) of MDR1 which are conserved in MDR1 P-gp from different species. Photoaffinity labeling experiments have suggested that this region directly interacts with the substrates of MDR1 (1, 2, 12, 13, 25). In mouse P-gp, replacing TM5 and TM6 with the homologous mdr2 segment is sufficient to abolish the colchicine and doxorubicin resistance conferred by mdr1 (3). The overall strategy of our work was to construct an inactive MDR1-MDR2 chimera and use it as a framework to reconstruct molecules with MDR1-like function by selectively replacing MDR2 residues with MDR1 residues. Our results indicate that Q330, V331, and L332 in TM6 of MDR1 P-gp are crucial for multidrug transporter activity and that with the exception of these residues, the amino-terminal half of the

* Corresponding author. Mailing address: Laboratory of Molecular Biology, National Cancer Institute, Building 37, Room 4E16, National Institutes of Health Bethesda, MD 20892. Phone: (301) 496-4797. Fax: (301) 402-1344. E-mail: pasta@helix.nih.gov.

MDR2 backbone, including the first six TM domains, can support multidrug transport.

MATERIALS AND METHODS

Mutagenesis and vector construction. A silent G-A substitution at bp 1185 was first introduced into MDR2 to create an *Eco*RI site at the same position as in MDR1. The MDR1-MDR2 chimera was constructed by exchanging homologous *Nsi*I/*Eco*RI digestion fragments. Two sets of mutations, (i) N330Q, A331V, and M332L and (ii) V364E, D367K, N372K, K374S, and E380K, were generated by a PCR mutagenesis method (17). MDR1, MDR1-MDR2(307–394), and MDR1-MDR2(307–394)QVL, as well as MDR1-MDR2(307–394)EKKSK, were inserted into the pHa retroviral vector at *Sac*II and *Xho*I sites (27).

Chimera MDR2(1–394)-MDR1 was constructed in the vaccinia virus pTM1 transient expression vector (9) downstream of the T7 promoter and the 5′-untranslated region, which included an internal ribosomal entry site, of the encephalomyocarditis virus as previously described (28). To obtain optimum expression, RNA transcription has to start from the *Nco*I site at the end of the 5′-untranslated region of encephalomyocarditis virus. The *Nco*I site in MDR2 was created at the ATG start codon by the PCR mutagenesis method. A three-way ligation was performed to link MDR2 (*Nco*I/*Sal*I, a PCR product), MDR2 (*Sal*I/*Eco*RI), and pTM1MDR1 (*Nco*I/*Eco*RI). In order to detect the expression of the chimeric protein MDR2(1–394)-MDR1 on the cell surface, a FLAG epitope containing octopeptide DYKDDDDK (Kodak) was inserted in the first extracellular loop between residues F98 and G99 of MDR2. The same FLAG epitope was also previously inserted in wild-type MDR1 between N94 and R95. MDR1-FLAG had identical characteristics to MDR1 based on fluorescence-activated cell sorter (FACS) analysis and iodoarylazidoprazosin (IAAP) photoaffinity labeling (17a). A *Sac*II site was also created by using PCR in the pTM1MDR2(1–394)-MDR1 chimera 37 bp before the MDR2 starting codon. Two sets of mutations, (i) N330Q, A331V, and M332L and (ii) V364E, D367K, N372K, K374S, and E380K were introduced into MDR2(1–394)-MDR1 by replacing the *Bam*HI/*Eco*RI fragment with the corresponding fragment of MDR1-MDR2(307–394)QVL, or MDR1-MDR2(307–394)EKKSK. The *Sac*II/*Xho*I fragment containing the entire MDR2(1–394)-MDR1 or MDR2(1–394)-MDR1QVL was inserted into the *Sac*II/*Xho*I site of the pHa retroviral vector. MDR1NAM was created by introducing mutations Q330N, V331A, and L332M into *MDR1* by PCR mutagenesis. All PCR products were sequenced to confirm that only the desired mutations were introduced.

Cell culture and DNA transfection. Both transient and stable protein expression approaches were employed in this work. Transient expression was based on the method developed by Moss and colleagues (9, 10, 26). cDNA was transcribed by this method from a T7 promoter by T7 RNA polymerase, which was expressed by a modified recombinant vaccinia virus (MVA). The cotransfection-infection procedure was performed as described previously by Ramachandra et al. (28). Briefly, 15 μg of DNA was mixed with 45 μl of Lipofectin (Life Technology, Inc.) in 3.5 ml of OptiMem medium and allowed to sit undisturbed at room temperature for 30 min. The mixture was then added to a 75-mm^2 flask preplated with 1.5×10^6 HeLa cells the night before. MVA was also added to the flask at 10^8 PFU/flask. After 4 h of incubation at 32°C, 12 ml of minimal essential medium containing 10% fetal bovine serum (FBS) was added. The cells were cultured at 32°C for another 18 h before the functional analysis.

Stable expression of MDR1 and its mutants were achieved by using a well-established pHa retroviral vector whose promoter is in the long terminal repeat of Harvey murine sarcoma virus (27). First, 10 μg of pHaMDR1(V185) or mutant DNA was cotransfected with 0.5 μg of pcDNA3 (Invitrogen) into NIH 3T3 cells by the calcium phosphate transfection method. pcDNA3 confers G418 resistance on the transfected cells through expression of *neo*. After selection for 7 days with 750 μg of G418 per ml, the surviving cells were pooled and labeled with anti-human MDR1 monoclonal antibody MRK-16 (14) at a concentration of 5 μg/5×10^5 cell in a volume of 200 μl at 4°C for 30 min. MRK-16-positive cells were isolated by using magnetic cell sorting with a miniMACS apparatus (Miltenyi Biotec GmbH). The MRK-16-positive cells were collected and expanded to 10^7. The aliquots of the expanded cells were stored in liquid nitrogen or analyzed either by a cytotoxicity assay or FACS.

FACS analysis of P-gp cell surface expression and fluorescent drug accumulation. The cell surface expression of MDR1 P-gp or its mutants was detected by using MDR1 monoclonal antibody MRK-16 (14) or, in some cases, M2 monoclonal antibody raised against the FLAG epitope (Kodak). About 2×10^5 to 3×10^5 cells were incubated in 200 μl of phosphate-buffered saline (PBS) containing 1% bovine serum albumin and 5 μg of MRK-16 or M2 antibody at 4°C for 30 min. After two washes with ice-cold PBS, the cells were further incubated with fluorescein isothiocyanate (FITC)-conjugated anti-mouse immunoglobulin G2a (IgG2a) or IgG1 monoclonal antibody (PharMingen) at 4°C for 45 min. The cells were then washed and analyzed with a FACSort apparatus equipped with Cellquest program (Becton Dickinson). The fluorescence intensity at the FL1 channel was plotted to compare the cell surface expression of MDR1 or its mutants.

In a fluorogenic substrate accumulation assay, 3×10^5 cells were incubated in 2 ml of phenol red-free Iscove medium (Life Technology, Inc.) which contained either 1 μg of bisantrene per ml, 3 μM daunomycin, or 0.5 μM rhodamine-123. After incubation at 37°C for 60 min, the cells were centrifuged, resuspended in ice-cold PBS, and analyzed by FACS. In some cases, after incubation with 0.5 μM rhodamine-123, the cells were incubated at 37°C in plain Iscove medium for 40 min before being analyzed by FACS.

Cell toxicity assay. The multidrug transporter activity of MDR1 or its mutants was also examined by using a cytotoxicity assay. Control NIH 3T3 cells resistant to G418 and NIH 3T3 cell populations expressing MDR1 or its mutants (positive for MRK-16 labeling, isolated by magnetic cell sorting) were plated at 10^3 cells/well in 96-well plates. On the second day, the cells were cultured in selective medium containing bisantrene, colchicine, daunomycin, or vincristine at a concentrations of 0, 0.3, 1, 3, 10, 30, 100, 300, or 1,000 ng/ml. After 72 h of incubation at 37°C, cell viability was determined with reagent WST-1 (an MTT analog from Boehringer Mannheim) according to the manufacturer's instruction. Triplicates of each sample were analyzed in this assay. The 50% inhibitory concentration (IC_{50}) was defined as the drug concentration required for 50% inhibition of the maximum WST-1 staining. The percentage of drug transporter activity of the MDR1 mutants versus the activity of wild-type MDR1 was calculated as $100 \times (IC_{50}\ [\text{mutant}] - IC_{50}\ [\text{neo}])/(IC_{50}\ [\text{MDR1}] - IC_{50}\ [\text{neo}])$.

Photoaffinity labeling with [^{125}I]IAAP. Aliquots of 5×10^5 HeLa cells transiently expressing MDR1, MDR1NAM, MDR2(1–394)-MDR1, MDR2(1–394)-MDR1QVL, and MDR2(1–394)-MDR1EKKSK were washed with ice-cold PBS and resuspended in 100 μl of PBS containing 7 nM [^{125}I]IAAP (Amersham) with or without 5 μM cyclosporin A or vinblastine at the indicated concentrations. The cell suspensions were incubated in the dark at room temperature for 60 min, followed by cross-linking under UV light at 366 nm for 30 min on ice. The cells were then washed once with ice-cold PBS, and the cell pellets were subjected to immunoprecipitation with anti-P-gp polyclonal antiserum PEPGα-13 as described previously (1, 2). The immunoprecipited samples were divided into two aliquots. One aliquot was analyzed by sodium dodecyl sulfate-polyacrylamide gel electrophoresis (SDS-PAGE) and used to detect labeled radioactivity; the other aliquot was subjected to immunoblotting analysis with C219 monoclonal antibody.

RESULTS

Sequence alignment of MDR1 and MDR2 between residues 307 and 394. A previous mutational study demonstrated that a mouse mdr1-mdr2 chimera containing TM5 and TM6 of mdr2 does not confer resistance to doxorubicin or colchicine (3), indicating that some of the replaced MDR1 residues are pivotal for multidrug transporter activity. To determine which residues within this region are essential for the multidrug transporter activity, we aligned the amino acid sequences of 10 mammalian MDR proteins (human MDR1 and MDR2; mouse mdr1, mdr2, and mdr3; rat mdr1 and mdr2; and Chinese hamster mdr1, mdr2, and mdr3) by using the Wisconsin Package software (Genetics Computer Group, Inc.). An alignment of the segment between residues 307 and 394 is shown in Fig. 1. Within this segment, 19 residues differ between human MDR1 and MDR2 P-gp (underlined in the MDR1 segment); 12 of these residues are conserved among the multidrug transporters (numbered). Based on an MDR1 TM organization model (5, 18, 19), these 12 residues are distributed as follows: two in the extracellular loop connecting TM5 and TM6 (T318 and S327), four in TM6 (Q330, V331, L332, and S351), and six in the cytoplasmic region following TM6 and preceding the N-terminal nucleotide binding domain (E353, E364, K367, K372, S374, and K380).

Functional analysis of MDR1-MDR2(307–394), MDR1-MDR2(307–394)QVL, and MDR1-MDR2(307–394)EKKSK. Our strategy to identify the essential MDR1 residues was to restore the multidrug transporter activity in MDR1-MDR2 chimeras by reintroducing selected MDR1 residues. The initial study was focused on the chimeric protein MDR1-MDR2(307–394). Two sets of mutations, (i) Q, V, and L at positions 330, 331, and 332 in TM6 or (ii) E, K, K, S, and K at positions 365, 367, 372, 374, and 380, respectively, within the cytoplasmic region, were introduced into MDR1-MDR2(307–394) to create MDR1-MDR2(307–394)QVL and MDR1-MDR2(307–394)EKKSK (Fig. 2). Functional characterization of the chimeras was performed with stably transfected NIH 3T3 cells. Retroviral vectors containing the gene encoding MDR1(V185), a well-characterized mutant of MDR1 (6, 28), or the MDR1-MDR2

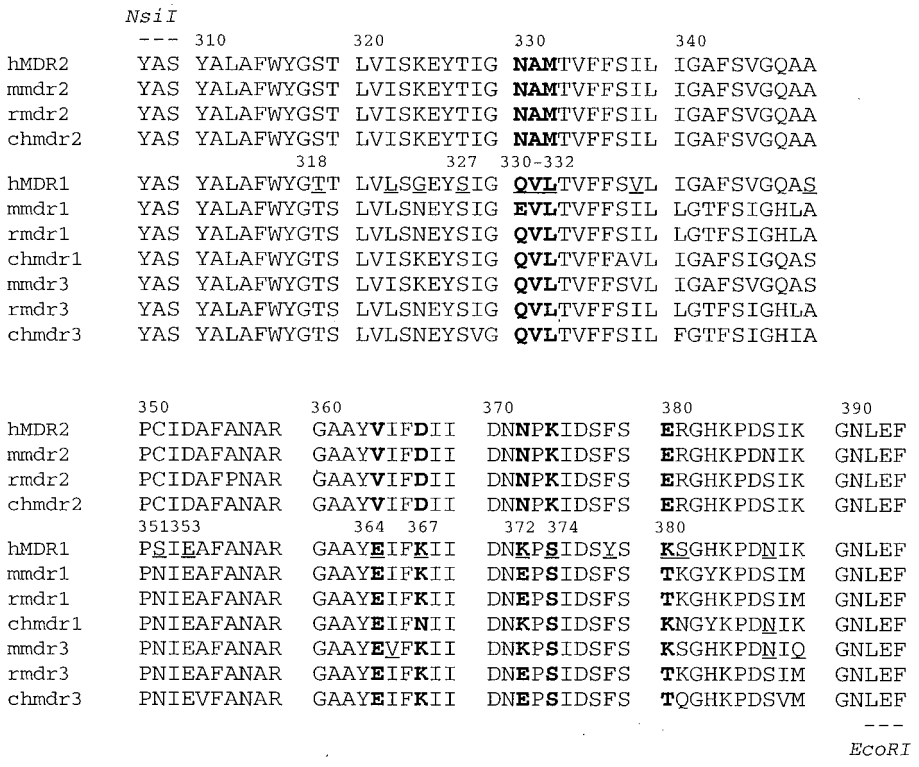

FIG. 1. Amino acid sequence alignment of mammalian MDR proteins between residues 307 and 394. The residues that differ between MDR1 and MDR2 are underlined. The residues in MDR1 differing from MDR2 but conserved in mdr1 and mdr3 are numbered with their position in MDR1. The residues studied in this work are in boldface. MDR prefixes: h, human; r, rat; ch, Chinese hamster; m, mouse.

chimera were cotransfected with pcDNA3, which confers G418 resistance. After G418 selection, the surviving cell population was pooled and incubated with monoclonal antibody MRK-16. The MRK-16-positive cells were isolated by a magnetic cell sorting method and used for functional studies.

Two approaches were used to compare the multidrug transporter activity of P-gp and its mutants. The first approach was to test the ability of MDR1-MDR2 chimeras to confer multidrug resistance in stably transfected NIH 3T3 cells. In this assay, the cells were exposed to cytotoxic drugs by using bisantrene, colchicine, daunomycin, or vincristine at various concentrations. The surviving cells were detected with the MTT analog WST-1. This assay scores the viable cells by detecting the enzymatic activity of functional mitochondria. As summarized in Table 1, MDR1-MDR2(307–394) conferred low-level bisantrene resistance compared to MDR1(V185), but it did not confer resistance to colchicine, daunomycin, and vincristine. Reintroducing MDR1 residues Q330, V331, and L332 into TM6 increased resistance to bisantrene and partially restored resistance to colchicine, daunomycin, and vincristine. Reintroducing E364, K367, K372, S374, and K380 into the cytoplasmic loop did not improve drug resistance. Similar results were also obtained by a direct cell colony formation assay (data not shown).

The second approach involved analyzing the transporter activity by a fluorogenic substrate accumulation assay. This assay takes advantage of the fact that some P-gp substrates have intrinsic fluorescence; the accumulation of these substrates can be determined by measuring the intracellular fluorescence by FACS analysis. Thus, this assay directly measures P-gp transporter activity. In this experiment we used fluorescent substrates rhodamine-123 and bisantrene. As shown in Fig. 3, the cells expressing MDR1-MDR2(307–394)QVL accumulated less bisantrene and rhodamine-123 than the cells expressing MDR1-MDR2(307–394) or MDR1-MDR2(307–394)EKKSK. These results indicate that reintroducing MDR1 residues Q330, V331, and L332 into TM6 of MDR1-MDR2(307–394) partially restored the transporter activity for bisantrene and rhodamine-123 but that reintroducing E364, K367, K372, S374, and K380 into the cytoplasmic region did not produce similar effects. Identical results were also obtained in an analysis of transiently expressed MDR1-MDR2 chimeras and wild-type MDR1 (data not shown).

The difference in drug transport could be due to a difference in the amount of P-gp on the cell surface. Therefore, we compared the cell surface expression of MDR1 with the MDR1-MDR2 chimeras by using MRK-16. The results indicate that over 90% of the sorted cells in the mass cell population are MRK-16 positive. MDR1(V185), MDR1-MDR2(307–394), and MDR1-MDR2(307–394)EKKSK were expressed on the cell surface at similar levels, but the expression of MDR1-MDR2(307–394)QVL was slightly less (Fig. 3). This difference may partially contribute to the lower transporter activity observed in the cells expressing MDR1-MDR2(307–394)QVL. In summary, both the cytotoxicity assay and the fluorescent substrate accumulation assays indicated that within the region containing residues 307 to 394, Q330, V331, and L332 in TM6 play a crucial role in sustaining multidrug transport activity, while S351, K367, K372, S374, and K380 in the cytoplasmic loop are less important.

Functional analysis of MDR2(1–394)QVL-MDR1 and MDR2(1–394)EKKSK-MDR1. To further investigate the significance of Q330, V331, and L332 in multidrug transporter activity, we examined the effects of these mutations in an MDR1-MDR2 chimera containing the entire MDR2 N-terminal transmembrane region (TM1-6; residues 1 to 394). Two sets of muta-

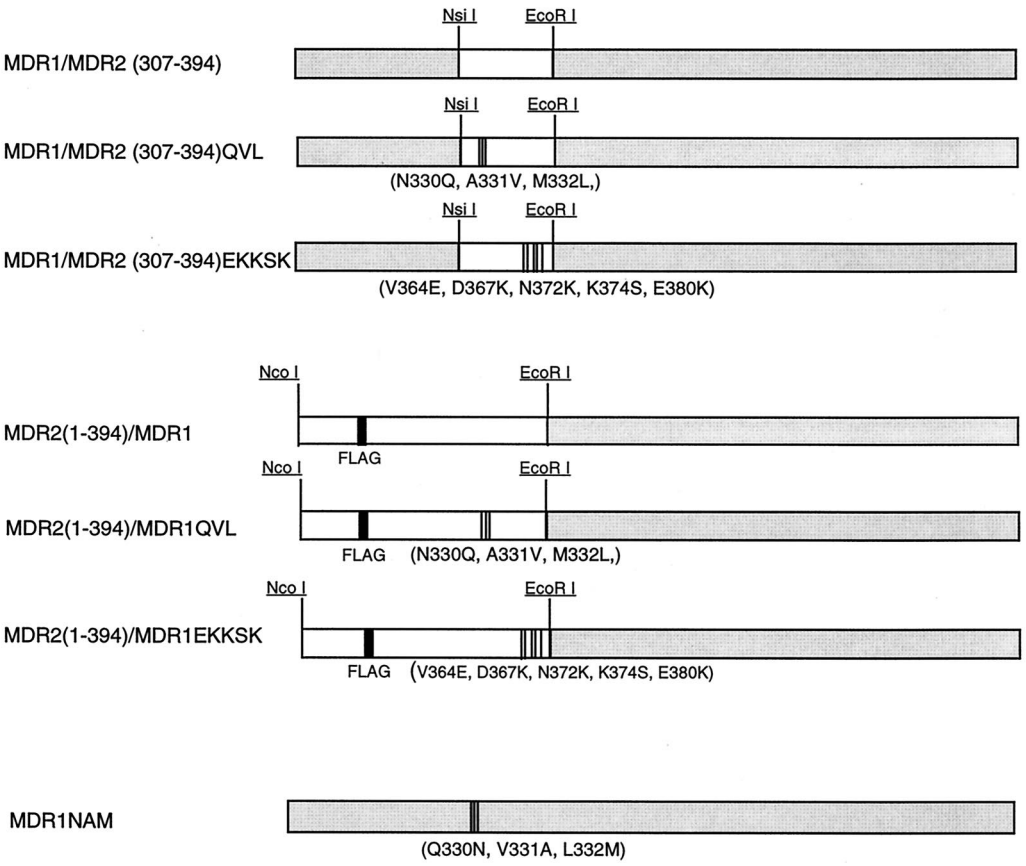

FIG. 2. Diagram of the chimeric MDR proteins. The FLAG epitope was inserted in MDR2 between F98 and G99. Open boxes, MDR2 segment; shaded boxes, MDR1 segment.

tions, (i) N330Q, A331V, and M332L and (ii) V364E, D367K, N372K, K374S, and E380K, were introduced into MDR2 (1–394)-MDR1 to generate MDR2(1–394)-MDR1QVL and MDR2(1–394)-MDR1EKKSK (Fig. 2). Since it was possible that the MRK-16 epitope would be missing in these MDR2-MDR1 chimeras, a FLAG epitope was inserted into the first extracellular loop of both chimeric and wild-type MDR1 to evaluate cell surface expression.

MDR2(1–394)-MDR1 and MDR2(1–394)-MDR1QVL were stably expressed in 3T3 cells. After G418 selection and magnetic cell sorting as described above, the mass population of MRK-16-positive cells was subjected to cytotoxicity assays. The results showed that MDR2(1–394)-MDR1 conferred low resistance to bisantrene and no resistance to colchicine, daunomycin, and vincristine. In comparison, MDR2(1–394)-MDR1 QVL conferred increased resistance to bisantrene and partial resistance to vincristine and colchicine; no resistance to daunomycin was observed (Table 2). The amounts of MDR1(V185), MDR2(1–394)-MDR1, and MDR2(1–394)-MDR1QVL proteins expressed on the cell surface were compared by labeling with monoclonal antibody raised against the FLAG epitope, followed by FACS analysis. MDR2(1–394)-MDR1QVL was expressed at a level comparable to wild-type MDR1, but MDR2 (1–394)-MDR1 was expressed at a somewhat lower level (data not shown).

To correct for the expression difference between MDR2 (1–394)-MDR1 and MDR2(1–394)-MDR1QVL in 3T3 cells, we transiently expressed both proteins, as well as MDR2(1–394)-MDR1EKKSK and MDR1, in HeLa cells by using a vaccinia virus-T7 RNA polymerase system. In comparison with other protein expression systems, the vaccinia virus-T7 RNA polymerase system enables one to achieve a high transfection efficiency and to produce large amounts of recombinant protein within a short period of time. The protein expressed on the cell surface was labeled by using a monoclonal antibody raised against the FLAG epitope and then detected by FACS. As shown in Fig. 4, the cells transfected with MDR1 or its mutants were separated into two populations. One population of cells was minimally fluorescent and thus similar to the cells transfected with the pTM1 vector, indicating that these cells did not express the MDR1-FLAG epitope. The other cell population was more fluorescent and equivalent, indicating that the cell surface expression of MDR2(1–394)-MDR1QVL and MDR2

TABLE 1. Relative drug resistance conferred by MDR1 or its mutants

MDR1 or mutant	Mean relative drug resistance[a] ± SE to:			
	Bisantrene	Colchicine	Daunomycin	Vincristine
neo	1	1	1	1
MDR1(V185)	12.2 ± 1.2	13.5 ± 0.1	4.3 ± 0.3	3.8 ± 0.8
MDR1-MDR2(307–392)	2.4 ± 0.5	1.2 ± 0.1	1.2 ± 0.2	1.4 ± 0.3
MDR1-MDR2(307–392)QVL	7.2 ± 1.3	8.4 ± 1.2	2.3 ± 0.3	2.2 ± 0.1
MDR1-MDR2(307–392)EKKSK	1.9 ± 0.2	2.1 ± 0.3	1.2 ± 0.4	1.1 ± 0.1

[a] The number represents the ratio of IC_{50} [MDR]/IC_{50} [neo].

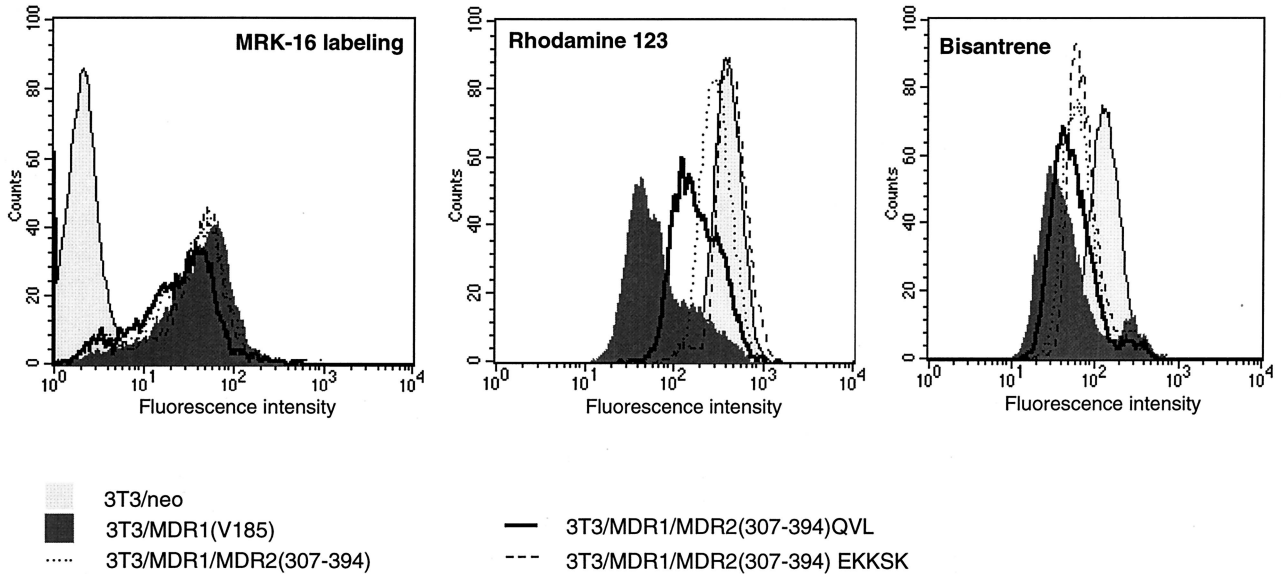

FIG. 3. Expression and function of MDR1-MDR2 chimeras after stable transfection. (A) The cell surface expression of MDR1, MDR1-MDR2(307–394), and its mutants on transfected 3T3 cells was determined by using MRK-16 antibody labeling and FACS analysis. The transporter activity of MDR1, MDR1-MDR2(307–394), and its mutants was analyzed by using a fluorescent substrate accumulation assay. The 3T3 cells expressing MDR1 or its mutants were incubated in medium containing 1 μg of bisantrene per ml (B) or 0.5 μM rhodamine-123 (C) at 37°C for 60 min. The fluorescence intensity, representing the intracellular accumulated substrate, was detected by FACS. Key: light gray areas, 3T3/neo; dark gray areas, 3T3/MDR1(V185); dotted line, 3T3/MDR1-MDR2(307–394); heavy line, 3T3/MDR1

(1–394)-MDR1EKKSE was at a level similar to wild-type P-gp. However, the expression of MDR2(1–394)-MDR1 was still slightly less than that of the other proteins.

The transport activities of transiently expressed MDR2(1–394)-MDR1QVL and MDR2(1–394)-MDR1EKKSK were determined by the fluorogenic substrate accumulation assay. Rhodamine-123, bisantrene, and daunomycin were used in this experiment. As shown in Fig. 4, the cells transfected with P-gp showed two populations. One population of cells, overlapping with the cells transfected with pTM1 vector, exhibited a high fluorescence intensity, indicating a lack of multidrug transporter activity. The second cell population had less fluorescence and was unique to the cells transfected with MDR1 or its mutants, indicating that the reduced fluorescence was associated with overexpression of MDR activity. MDR2(1–394)-MDR1QVL exhibited efflux activity for bisantrene and rhodamine-123 but not for daunomycin. MDR2(1–394)-MDR1 EKKSK showed low-level efflux activity for bisantrene but no efflux activity for rhodamine-123 or daunomycin. This result suggests that substituting residues Q330, V331, and L332 in MDR2(1–394)-MDR1 can improve multidrug transporter activity in MDR1-MDR2 chimeras, though the transporter efficiency varies with the substrate tested.

Previous studies showed that a mouse mdr2(1–394)-mdr1 chimera does not confer doxorubicin and colchicine resistance in a stable transfected cell line (3). We obtained similar results with human P-gp chimeras. However, with either the stable or the transient expression systems, we were not able to express this protein on the cell surface at a level equivalent to the wild-type P-gp or MDR2(1–394)-MDR1QVL. The low-level expression of MDR2(1–394)-MDR1 observed in this experiment may be related to an inhibitory effect of the MDR2 coding sequence on protein expression, since full-length MDR2 P-gp is also expressed at a lower level than MDR1 in either stable or transient expression systems (4, 35). Because MDR2(1–394)-MDR1 was expressed at a lower level than MDR2(1–394)-MDR1QVL, it is difficult to directly compare their transport activities. However, the importance of Q330, V331, and L332 in MDR2(1–394)-MDR1 can be demonstrated through comparison of the transporter activities of MDR2(1–394)-MDR1 QVL and MDR2(1–394)-MDR1EKKSK.

Expression and functional analysis of MDR1NAM. To confirm the significance of Q330, V331, and L332 in TM6, we generated a MDR1 mutant containing the mutations Q330N, V331A, and L332M. This MDR1 mutant, MDR1NAM, was transiently expressed in HeLa cells by using a vaccinia virus-T7 expression system as described above. The cell surface expression of MDR1 and MDR1NAM were compared by labeling intact cells with P-gp monoclonal antibody MRK-16. The multidrug transporter activity of MDR1NAM was compared with MDR1 by using a fluorogenic substrate accumulation assay. Bisantrene, rhodamine-123, and daunomycin were tested. We found that although MDR1NAM was expressed on the cell surface as much as the wild-type MDR1, its capacity to efflux daunomycin was almost lost and the activity to efflux bisantrene, calcein AM, and rhodamine-123 were also significantly reduced but not abrogated (Fig. 5). Similar results were also obtained with 3T3 cells that stably expressed MDR1NAM. Compared to MDR1(V185), MDR1NAM conferred 49% as much resistance to bisantrene and 22% as much resistance to daunomycin. These results suggest that Q330, V331, and L332

TABLE 2. Relative drug resistance conferred by MDR1 or its mutants

MDR1 or mutant	Mean relative drug resistance[a] ± SE to:			
	Bisantrene	Colchicine	Daunomycin	Vincristine
neo	1	1	1	1
MDR1(V185)	12.2 ± 1.2	13.5 ± 0.1	4.3 ± 0.3	3.8 ± 0.8
MDR2(1–394)-MDR1	2.4 ± 0.6	1.2 ± 0.1	0.9 ± 0.2	1.0 ± 0.1
MDR2(1–394)-MDR1QVL	7.6 ± 1.8	4.5 ± 0.1	1.4 ± 0.3	1.8 ± 0.1

[a] The number represents the ratio of IC_{50} [MDR]/IC_{50} [neo].

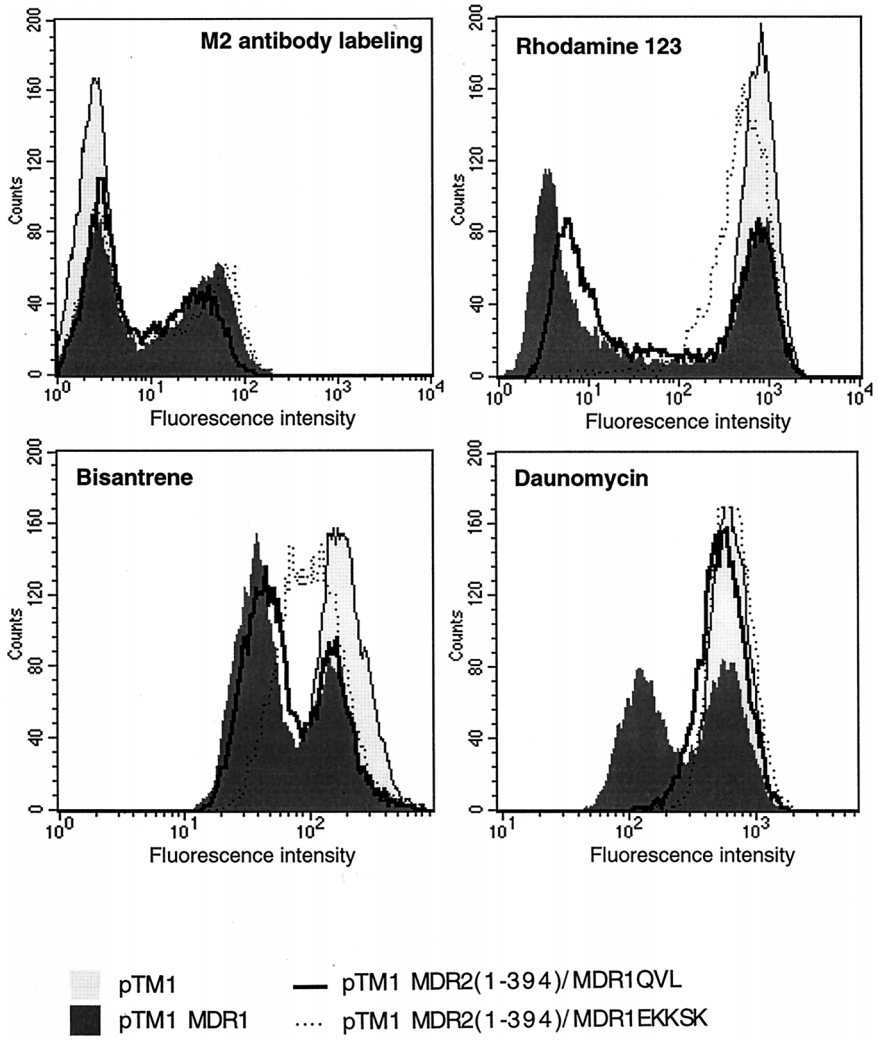

FIG. 4. Expression and function analysis of transiently expressed MDR2(1–394)-MDR1 and its mutants. MDR2(1–394)-MDR1, MDR2(1–394)/MDR1QVL and MDR2(1–394)/MDR1EKKSK were transiently expressed in HeLa cells. The cell surface-expressed protein was labeled by using a monoclonal antibody raised against the FLAG epitope followed by FACS analysis. Transporter activity of MDR2(1–394)-MDR1QVL and MDR2(1–394)-MDR1EKKSK was analyzed by a fluorescent substrate accumulation assay. The HeLa cells transfected with MDR1 or its mutants were incubated in medium containing 1 μg of bisantrene per ml, 0.5 μM rhodamine-123, or 3 μM daunomycin at 37°C for 60 min. The cells incubated with rhodamine-123 were further incubated in rhodamine-123-free medium at 37°C for another 45 min. The fluorescence intensity, representing the intracellular accumulated substrate, was detected by FACS. To better show the difference between two cell populations, a zoom-in version of the FACS result is used for the bisantrene and daunomycin panels.

are quantitatively important for overall multidrug transporter activity of MDR1.

Photoaffinity labeling of MDR1, MDR2(1–394)-MDR1, MDR2(1–394)-MDR1 QVL, and MDR2(1–394)-MDR1 EKKSK. To determine whether the change of multidrug transporter activity of MDR1-MDR2 chimeras was related to a change in their ability to interact with substrate, we performed photoaffinity labeling experiments with IAAP. The HeLa cells transiently expressing MDR1, MDR1NAM, MDR1-MDR2(1–394), MDR1-MDR2(1–394)QVL, or MDR1-MDR2(1–394) EKKSK were incubated with 7 nM IAAP, a concentration below the K_m of wild-type MDR1, in the presence or absence of 5 μM cyclosporin A. After photoaffinity labeling, P-gp was immunoprecipitated and separated by SDS-PAGE. The radioactive label on P-gp was measured by using the STORM system (Fig. 6A). We found that MDR1 and all of the MDR1-MDR2 chimeras could be labeled with IAAP and that this IAAP labeling was blocked by the MDR1 reversing-agent cyclosporin A. After normalization to the relative amount of P-gp with Western blotting analysis, we calculated a relative IAAP labeling efficiency for each sample. These data showed that as compared to MDR1 (100%), the relative specific IAAP labeling efficiencies of MDR1NAM, MDR2(1–394)-MDR1, MDR2(1–394)-MDR1QVL, or MDR2(1–394)-MDR1EKKSK were 68, 37, 85, or 90%, respectively (Fig. 6B). Like mouse mdr2 (4), human MDR2 was only nonspecifically photoaffinity labeled at low level with IAAP (data not shown). Using IAAP labeling as an indicator, we also determined whether the MDR1-MDR2 chimeras could interact with the P-gp substrate vinblastine by determining if vinblastine would competitively block IAAP labeling. We found that IAAP labeling of MDR2 (1–394)-MDR1 was blocked by vinblastine in a dose-dependent manner (Fig. 7). Furthermore, MDR2(1–394)-MDR1 QVL and MDR2(1–394)-MDR1EKKSK were even more sensitive than MDR1 to a low concentration of vinblastine. These results indicate a relatively normal interaction between vinblastine and MDR1-MDR2 chimeras.

Our previous work demonstrated that *cis*-fluopentixol stim-

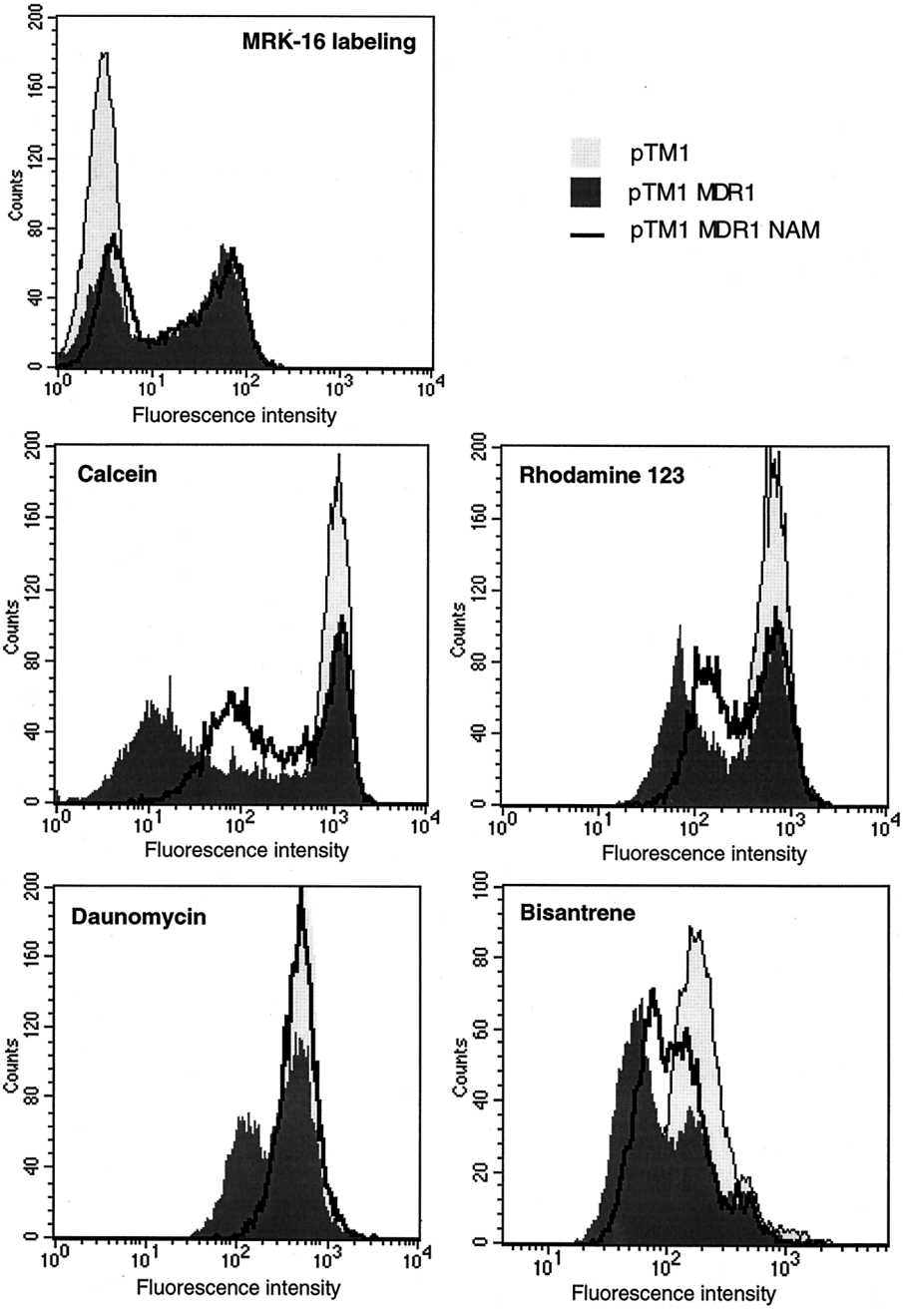

FIG. 5. Functional analysis of MDR1NAM. MDR1NAM and MDR1 were transiently expressed in HeLa cells. The cell surface expression of each protein was compared by MRK-16 labeling followed by FACS analysis. The transport activity of transiently expressed MDR1NAM was analyzed by fluorescent substrate accumulation assay at a final concentration of 1 μM bisantrene, 0.5 μM rhodamine-123, or 3 μM daunomycin. A zoom-in version of the FACS result is used for the bisantrene panel.

ulates IAAP photoaffinity labeling of MDR1 through binding to the second drug-binding site (8). To determine whether MDR1 residues in TM6 are involved in forming the second drug-binding site, we performed IAAP labeling of various MDR1-MDR2 chimeras in the presence or absence of *cis*-fluopentixol. We found that *cis*-fluopentixol stimulated IAAP labeling of MDR1-MDR2(307–394)QVL and MDR1-MDR2 (307–394)EKKSK but not of MDR2(1–394)-MDR1QVL or MDR2(1–394)-MDR1EKKSK (data not shown). These results suggest that MDR1 N-terminal residues 1 to 307 are essential for the second drug (*cis*-fluopentixol) binding site.

DISCUSSION

Determination of the residues in P-gp essential for the transport of specific drugs offers the promise of defining substrate binding domains in this energy-dependent multidrug transporter. Using an approach involving exchanging homologous segments of MDR1 and MDR2 and site-directed mutagenesis, we demonstrated that MDR1 residues Q330, V331, and L332 in TM6 were essential for multidrug transporter activity. Substituting Q330, V331, and L332 with MDR2 residues could significantly impair MDR1 activity, while the triple mutation

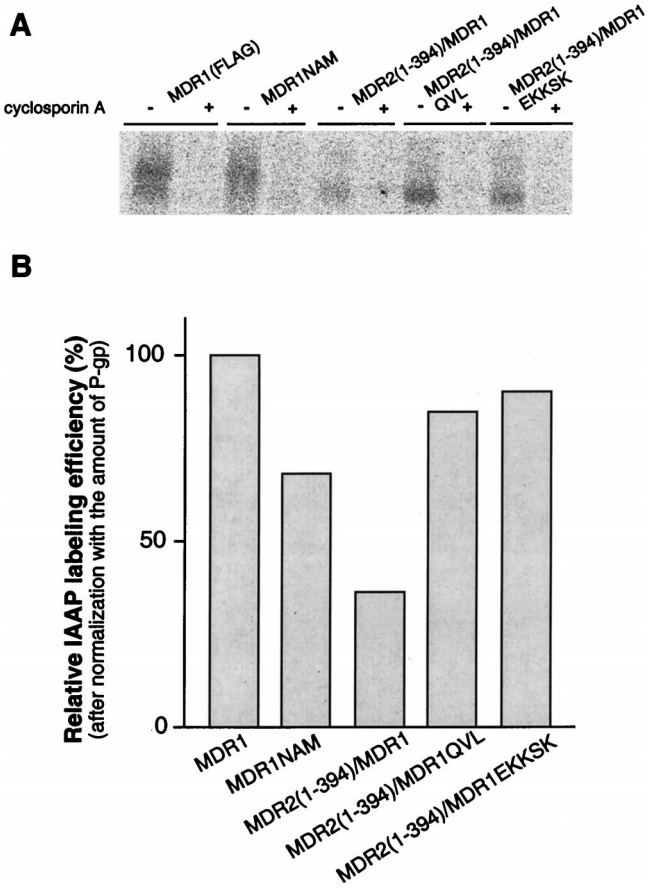

FIG. 6. IAAP photoaffinity labeling of MDR1, MDR1NAM, MDR2(1–394)-MDR1, MDR2(1–394)-MDR1QVL, and MDR2(1–394)/MDR1EKKSK. A total of 500,000 HeLa cells transiently expressing MDR1 and its mutants were incubated with 7 nM [^{125}I]IAAP in 100 μl of PBS with or without 5 μM cyclosporine A at room temperature for 60 min, followed by cross-linking with UV at 366 nm for 30 min on ice. (A) The P-gps were immunoprecipitated with P-gp polyclonal antibody PEPGα-13 and analyzed by SDS-PAGE. (B) The radioactivity associated with the P-gp band was measured and quantitated by using the STORM system. After normalization to the relative amount of P-gp in each sample, the relative IAAP specific labeling efficiency is shown. The relative IAAP specific labeling efficiency of MDR1 P-gp is shown as 100%.

N330Q A331V M332L was sufficient to allow the MDR2 TM domain (residues 307 to 394 or residues 1 to 394) in the N-terminal half of P-gp to support multidrug transporter activity. These results suggest structural and functional similarity between the multidrug transporter and phosphatidylcholine flippase.

Identification of Q330, V331, and L332 as the critical residues for the multidrug transporter activity. To identify the essential residues for MDR1 broad substrate specificity, we focused on the residues conserved only among MDR multidrug transporters, while omitting residues conserved in MDR1 and MDR2. The latter conserved residues are assumed to be structurally or functionally important for both multidrug transporter and phosphatidylcholine flippase, but they do not determine the broad multidrug recognition of P-gp. Construction of MDR1-MDR2 chimeras allowed us to investigate the role of some unique residues for multidrug transporter and to determine the residues responsible for the functional differences between the multidrug transporter and phosphatidylcholine flippase.

Identification of Q330, V331, and L332 as the critical residues for the multidrug transporter was based on two lines of evidence. One is that the substitutions Q330N, V331A, and L332M in MDR1 significantly decreased overall MDR1 multidrug transporter activity. The other is that substituting N330Q, A331V, and M332L in the MDR2 region of either MDR2 (307–394)-MDR1 or MDR2(1–394)-MDR1 partially restored the lost MDR1 function in the MDR1-MDR2 chimeras. Even though the restored activity was somewhat less than the activity of MDR1, depending on the individual substrate tested, the effects of Q330, V331, and L332 on the MDR1-MDR2 chimeric proteins are significant, considering they represent less than 16% (3/19) of the differences between MDR1 and MDR2 within the region from TM5 to TM6 (307 to 394), and 2.5% (3/121) of the differences within the region from TM1 to TM6 (1 to 394). The ability to restore the multidrug transport activity of MDR1-MDR2 chimeras is unique to Q330, V331, and L332, since residues E364, K367, K372, S374, and K380 within the cytoplasmic region did not produce similar effects. In addition, the introduction of either residues E364, K367, K372, S374, and K380 or residues T318, L322, G324, and S327 into MDR1-MDR2(307–394)QVL did not further improve the multidrug transport activity, implying that these residues may not significantly contribute to drug transport (data not shown). It should be pointed out that N-Q and M-L have very similar chemical properties and that they are often interchangeable among proteins with the same biological function. Therefore, it is possible that the functional difference made by mutations N-Q, A-V, and M-L is due to their unique structural location rather than to their chemical differences.

Mutations at residues 330, 331, and 332 produce quantitative effects on multidrug transport activity. Although Q330, V331, and L332 are important for the broad substrate spectrum of P-gp, these results do not exclude the possibility that other residues, including the residues conserved in both MDR1 and MDR2, are essential for the interaction with P-gp substrates. In fact, both MDR1-MDR2(307–394) and MDR2 (1–394)-MDR1 have residual ability to efflux bisantrene but not enough to support multidrug transport unless Q330, V331, and L332 are present. On the other hand, residues Q330, V331, and L332 are not absolutely necessary for multidrug transporter activity. Substituting Q330, V331, and L332 with MDR2 residues in an MDR1 backbone decreased but did not abolish overall multidrug transport activity. These results suggest that multiple factors may be involved in sustaining multidrug transporter activity, and each factor can function independently. In addition, earlier mutational studies showed that replacing Q330, V331, or L332 individually with Ala or Cys has no significant effects on MDR activity (20–22). However, by simultaneously replacing Q330, V331, and L332 with Ala, we observed an overall reduced MDR1 activity similar to MDR1 NAM (data not shown). Thus, the triple mutation Q330N, V331A, and L332M appeared to have a synergistic effect. Similar observations have also been made recently in studies on substitutions of nonconserved MDR1 residues in TM12 (15). We do not know whether all three residues are important, or whether any two of them might have the same effect. Taken together, we believe that the effects of Q330, V331, and L332 on multidrug transport are quantitatively significant.

Mutations at residues 330, 331, and 332 may cause a change in P-gp conformation. It is not yet clear why Q330, V331, and L332 are important for multidrug transporter activity. In an IAAP photoaffinity labeling experiment, we observed that all the MDR1-MDR2 chimeras were labeled by IAAP and that this IAAP labeling was blocked by the P-gp inhibitor cyclosporin A. Although the restoration or loss of MDR1 activity in MDR1-MDR2 chimeras roughly paralleled the increase or decrease in IAAP binding, the changes in IAAP labeling are

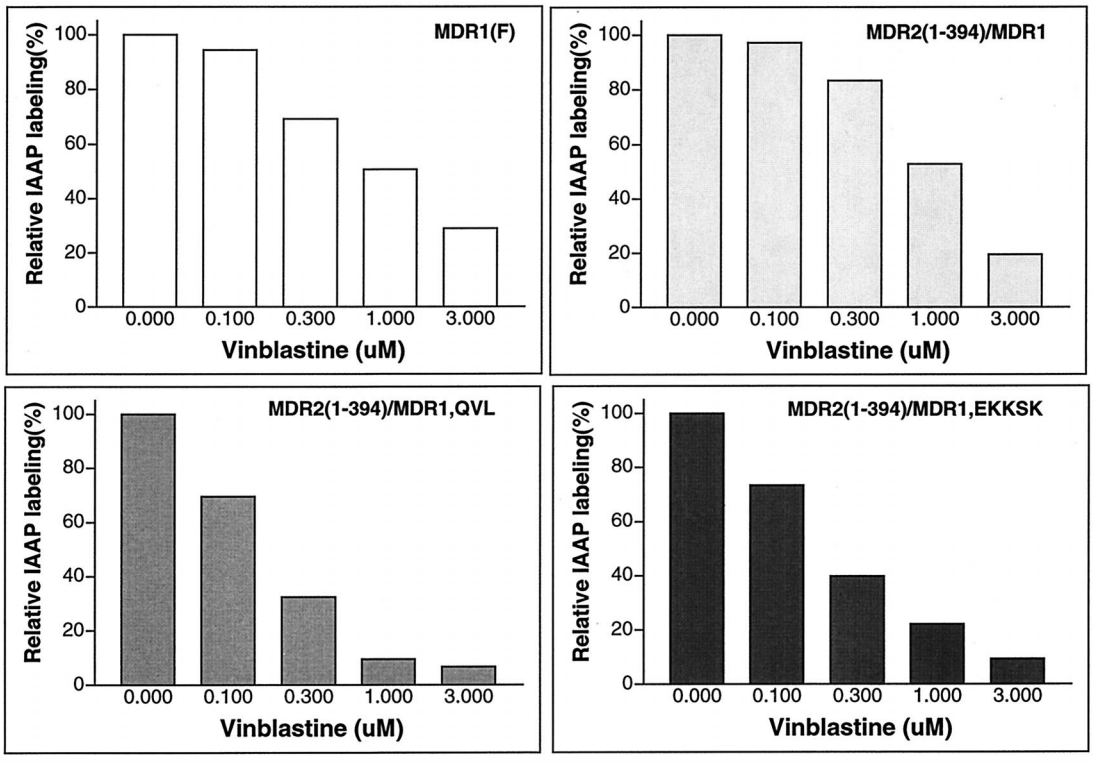

FIG. 7. IAAP photoaffinity labeling in the presence of various concentrations of vinblastine. IAAP labeling was carried out as described above in the presence of vinblastine at concentrations of 0, 0.1, 0.3, 1, and 3 μM. After immunoprecipitation and SDS-PAGE separation, the radioactivity associated with P-gp was measured and quantitated by using the STORM system. The normalized IAAP labeling is shown. The relative IAAP labeling in the absence of vinblastine is shown as 100%.

not quantitatively correlated with the changes in multidrug transporter activity. Furthermore, we found that vinblastine blocked IAAP labeling of all the MDR1-MDR2 chimeras in a dose-dependent manner, even though MDR2(1–394)-MDR1 and MDR2(1–394)-MDR1EKKSK displayed little ability to efflux [^{3}H]vinblastine (data not shown). This finding is similar to a previous observation that a nonfunctional MDR1 mutant carrying a mutation in TM6 displays rather normal drug-binding affinity. In that case the mutated residue, S344, is conserved in both MDR1 and MDR2 (20).

Taken together, these results suggest that Q330, V331, and L332 may be involved in the interaction between MDR1 and its substrates but perhaps not by directly binding substrates. Based on the finding that substitutions of residues 330, 331, and 332 in TM6 did not fully eliminate MDR1 function, we speculate that these three residues are structurally important; mutations that occurred at these positions may cause a conformational change which not only affects MDR1 substrate interaction but also changes other unknown steps in the drug transport process. This hypothesis is plausible in light of a recent study which demonstrates that movement between TM6 and TM12 is essential for drug-stimulated ATP hydrolysis and drug transport and that interaction between L332 and L975 is involved in this process (22). In a recent study, we found that in the absence of P-gp substrate, MDR1NAM bound to UIC2, a conformation-sensitive monoclonal antibody against P-gp (23, 24), less well than wild-type MDR1, but that this difference was eliminated by the presence of a P-gp substrate (35). Since the UIC2 epitope depends on a particular P-gp conformation (24), the decreased level of UIC2 recognition may indicate a conformational change in MDR1 caused by mutations Q330N, V331A, and L332M.

Implications for mechanism of action of P-gp. The multidrug transporter has been suggested to be a "hydrophobic vacuum cleaner" (29) or a "multidrug flippase" (16), owing to its apparent ability to remove drugs directly from the lipid bilayer. This concept was reenforced by the discovery that the closely related MDR2 gene product is indeed a phosphatidylcholine flippase (31) and that MDR1 is also able to translocate short-chain phospholipids (33). The results presented here show that the entire amino-terminal TM domain from MDR2 can support multidrug transport with substitution of only three amino acid residues, suggesting that structural differences between MDR1 and MDR2 in the N-terminal TM region are much smaller than the approximately 30% differences observed in their amino acid sequences. This structural similarity provides further evidence for the essential mechanistic similarities of these two transporters. Whether this reflects some association of hydrophobic drug substrates of the P-gp transporter with membrane lipid or the direct recognition of drugs intercalated within the plasma membrane remains to be determined. It would be interesting to determine if MDR2 residues in MDR1 can confer phosphatidylcholine flippase activity on MDR1. However, this assay is technically difficult, and we have not been able to perform it.

The ability of the N-terminal TM domain of MDR2 to support multidrug transport is even more surprising in light of previous results that segments of MDR2 in the amino-terminal TM region cannot support MDR1 function even when MDR1 TM6 is preserved (3, 7). The current results suggest that MDR2 residues can function in the context of other MDR2 residues, but not of MDR1 residues, in the amino-terminal TM domain. The simplest interpretation of these results is that the amino-terminal TM domain of MDR2 forms a structure capable of

supporting MDR1 function if and only if interaction between MDR2 residues is possible. Thus, the requirement for the folding of the amino-terminal TM domains of MDR1 and MDR2 would appear to be more MDR type specific than the requirement for interaction of the amino- and carboxyl-terminal TM domain of the P-gp, except perhaps in TM6.

The results reported here provide important information for understanding how drugs and inhibitors interact with P-gp and the molecular basis of the difference between the multidrug transporter and phosphatidylcholine flippase. These data will help in the design of new drugs to reverse drug resistance caused by P-gp. The ability to dramatically modify the substrate specificity of P-gp by substitution of a few amino acid residues also allows us to design transporters with special properties for use as selectable markers in human gene therapy (11).

ACKNOWLEDGMENTS

We are grateful to Christine Hrycyna for providing pTM1 MDR1 (FLAG) plasmid and to Bernard Moss for providing the MVA vaccinia virus.

REFERENCES

1. **Bruggemann, E. P., U. A. Germann, M. M. Gottesman, and I. Pastan.** 1989. Two different regions of P-glycoprotein are photoaffinity labeled by azidopine. J. Biol. Chem. **264:**15483–15488.
2. **Bruggemann, E. P., S. J. Currier, M. M. Gottesman, and I. Pastan.** 1992. Characterization of the azidopine and vinblastine binding site of P-glycoprotein. J. Biol. Chem. **267:**21020–21026.
3. **Buschman, E., and P. Gros.** 1991. Functional analysis of chimeric genes obtained by exchanging homologous domains of the mouse *mdr1* and *mdr2* genes. Mol. Cell. Biol. **11:**595–603.
4. **Buschman, E., and P. Gros.** 1994. The inability of the mouse *mdr2* gene to confer multidrug resistance is linked to reduced drug binding to the protein. Cancer Res. **54:**4892–4898.
5. **Chen, C.-J., J. E. Chin, K. Ueda, D. Clark, I. Pastan, M. M. Gottesman, and I. B. Roninson.** 1986. Internal duplication and homology with bacterial transport proteins in the *mdr1* (P-glycoprotein) gene from multidrug-resistant human cells. Cell **47:**381–389.
6. **Choi, K., C.-J. Chen, M. Kriegler, and B. Roninson.** 1989. An altered pattern of cross-resistance in multidrug-resistant human cells results from spontaneous mutations in the mdr1 (P-glycoprotein). Cell **53:**519–529.
7. **Currier, S. J., S. E. Kane, M. C. Willingham, C. O. Cardarelli, I. Pastan, and M. M. Gottesman.** 1992. Identification of residues in the first cytoplasmic loop of P-glycoprotein involved in the function of chimeric human MDR1-MDR2 transporters. J. Biol. Chem. **267:**25153–25159.
8. **Dey, S., M. Ramachandra, I. Pastan, M. M. Gottesman, and S. V. Ambudkar.** 1997. Evidence for non-identical drug interaction sites in the human P-glycoprotein. Proc. Natl. Acad. Sci. USA **94:**10594–10599.
9. **Elroy-Stein, O., T. R. Fuerst, and B. Moss.** 1989. Cap-independent translation of mRNA conferred by encephalomyocarditis virus 5′ sequence improves the performance of the vaccinia virus/bacteriophage T7 hybrid expression system. Proc. Natl. Acad. Sci. USA **86:**6126–6130.
10. **Fuerst, T. R., E. G. Niles, F. W. Studier, and B. Moss.** 1986. Eukaryotic transient-expression system based on recombinant vaccinia virus that synthesizes bacteriophage T7 RNA polymerase. Proc. Natl. Acad. Sci. USA **83:**8122–8126.
11. **Gottesman, M. M., C. A. Hrycyna, P. V. Schoenlein, U. A. Germann, and I. Pastan.** 1995. Genetic analysis of the multidrug transporter. Annu. Rev. Genet. **29:**607–649.
12. **Greenberger, L. M., C. J. Lisanti, J. T. Silva, and S. B. Horwitz.** 1991. Domain mapping of the photoaffinity drug-binding sites in P-glycoprotein encoded by mouse mdr1b. J. Biol. Chem. **266:**20744–20751.
13. **Greenberger, L. M.** 1993. Major photoaffinity drug labeling sites for iodoaryl azidoprazosin in P-glycoprotein are within, or immediately C-terminal to, transmembrane domains 6 and 12. J. Biol. Chem. **268:**11417–11425.
14. **Hamada, H., and T. Tsuruo.** 1986. Functional role for the 170- to 180-kDa glycoprotein specificto drug-resistant tumor cells as revealed by monoclonal antibodies. Proc. Natl. Acad. Sci. USA **83:**7785–7789.
15. **Hefkemeyer, P., S. Dey, S. V. Ambudkar, C. A. Hrycyna, I. Pastan, and M. M. Gottesman.** 1998. Contribution to substrate specificity and transport of nonconserved residues in transmembrane domain 12 of human P-glycoprotein. Biochemistry **37:**16400–16409.
16. **Higgins, C. F., and M. M. Gottesman.** 1992. Is the multidrug transporter a flippase? Trends Biochem. Sci. **17:**18–21.
17. **Higuchi, R.** 1992. Pages 61–70. *In* H. A. Erlich (ed.), PCR technology. W. H. Freeman and Company, New York, N.Y.

17a. **Hrycyna, C., I. Pastan, and M. M. Gottesman.** Unpublished data.

18. **Kast, C., V. Canfield, R. Levenson, and P. Gros.** 1995. Membrane topology of P-glycoprotein as determined by epitope insertion: transmembrane organization of the N-terminal domain of mdr3. Biochemistry **34:**4402–4411.
19. **Kast, C., V. Canfield, R. Levenson, and P. Gros.** 1996. Transmembrane organization of mouse P-glycoprotein determined by epitope insertion and immunofluorescence. J. Biol. Chem. **271:**9240–9248.
20. **Loo, T. W., and D. M. Clarke.** 1994. Mutations to amino acids located in predicted transmembrane segment 6 (TM6) modulate the activity and substrate specificity of human P-glycoprotein. Biochemistry **33:**14049–14057.
21. **Loo, T. W., and D. M. Clarke.** 1996. Inhibition of oxidative cross-linking between engineered cysteine residues at positions 332 in predicted transmembrane segments (TM) 6 and 975 in predicted TM12 of human P-glycoprotein by drug substrates. J. Biol. Chem. **271:**27482–27487.
22. **Loo, T. W., and D. M. Clarke.** 1997. Drug-stimulated ATPase activity of human P-glycoprotein requires movement between transmembrane segments 6 and 12. J. Biol. Chem. **272:**20986–20989.
23. **Mechetner, E. B., and I. B. Roninson.** 1992. Efficient inhibition of P-glycoprotein-mediated multidrug resistance with a monoclonal antibody. Proc. Natl. Acad. Sci. USA **89:**5824–5828.
24. **Mechetner, E. B., B. Schott, B. Morse, W. D. Sten, T. Druley, K. A. Davis, T. Tsuruo, and I. B. Roninson.** 1997. P-glycoprotein function involves conformational transitions detectable by differential immunoreactivity. Proc. Natl. Acad. Sci. USA **94:**12908–12913.
25. **Morris, D. I., L. M. Greenberger, E. P. Bruggemann, C. Cardarelli, M. M. Gottesman, I. Pastan, and K. B. Seamon.** 1994. Localization of the forskolin labeling sites to both halves of P-glycoprotein: similarity of the sites labeled by forskolin and prazosin. Mol. Pharmacol. **46:**329–337.
26. **Moss, B.** 1991. Vaccinia virus: a tool for research and vaccine development. Science **252:**1662–1667.
27. **Pastan, I., M. M. Gottesman, K. Ueda, E. Lovelace, A. V. Rutherford, and M. C. Willingham.** 1988. A retrovirus carrying an MDR1 cDNA confers multidrug resistance and polarized expression of P-glycoprotein in MDCK cells. Proc. Natl. Acad. Sci. USA **85:**4486–4490.
28. **Ramachandra, M., S. Ambudkar, M. M. Gottesman, I. Pastan, and C. A. Hrycyna.** 1996. Functional characterization of a glycine 185 to valine substitution in human P-glycoprotein using a vaccinia based transient expression system. Mol. Biol. Cell **7:**1485–1498.
29. **Raviv, Y., H. B. Pollard, E. P. Bruggemann, I. Pastan, and M. M. Gottesman.** 1990. Photosensitized labeling of a functional multidrug transporter in living drug-resistant tumor cells. J. Biol. Chem. **265:**3975–3980.
30. **Ruetz, S., and P. Gros.** 1994. Phosphatidylcholine translocase: a physiological role for the mdr2 gene. Cell **77:**1071–1081.
31. **Smit, J. J., A. H. Schinkel, R. P. Oude-Elferink, A. K. Groen, E. Wagenaar, L. van Deemter, C. A. Mol, R. Ottenhoff, N. M. van der Lugt, M. A. van Roon, et al.** 1993. Homozygous disruption of the murine mdr2 P-glycoprotein gene leads to a complete absence of phospholipid from bile and to liver disease. Cell **75:**451–462.
32. **van der Bliek, A. M., P. M. Kooiman, C. Schneider, and P. Borst.** 1988. Sequence of mdr3 cDNA encoding a human P-glycoprotein. Gene **71:**401–411.
33. **van Helvoort, A., A. J. Smith, H. Sprong, I. Fritzsche, A. H. Schinkel, P. Borst, and G. van Meer.** 1996. MDR1 P-glycoprotein is a lipid translocase of broad specificity, while MDR3 P-glycoprotein specifically translocates phosphatidylcholine. Cell **87:**507–517.
34. **Zhang, X., K. I. Collins, and L. M. Greenberger.** 1995. Functional evidence that transmembrane 12 and the loop between transmembrane 11 and 12 form part of the drug-binding domain in P-glycoprotein encoded by MDR1. J. Biol. Chem. **270:**5441–5448.
35. **Zhou, Y., M. M. Gottesman, and I. Pastan.** Unpublished data.